HIL Emulation of All-Electric UAV Power Systems

Rebecca Todd
Member, IEEE
Rolls-Royce UTC
School of Electrical & Electronic Eng.
The University of Manchester
Manchester, M60 1QD, UK
rebecca.todd@manchester.ac.uk

Andrew J. Forsyth
Member, IEEE
Rolls-Royce UTC
School of Electrical & Electronic Eng.
The University of Manchester
Manchester, M60 1QD, UK
andrew.forsyth@manchester.ac.uk

Abstract -- **Hardware-in-the-loop (HIL) techniques are used to examine the start-up sequence for an all-electric UAV system powered by a two-spool gas engine with embedded electrical generators on both spools. Start-up begins with the auxiliary power unit charging the high voltage DC bus to enable the high pressure spool switched reluctance starter/generator (SRSG) to spin the gas engine to ground idle speed and ends with the SRSG and the low pressure spool fault-tolerant permanent magnet generator being connected in parallel. HIL methods are used to emulate the behaviour of the gas engine and the loads. The HIL elements compliment the 'real' electrical generators and bus system. The start-up sequence is demonstrated on a purpose-built laboratory system to examine system interactions and the feasibility of the operating routine.**

***Index Terms*—Hardware-in-the-loop, All-electric aircraft, Uninhabited autonomous vehicle.**

I. NOMENCLATURE

AEA	All-electric aircraft
ALS	Active load systems
APU	Auxiliary power unit
FCS	Flight control system
HIL	Hardware-in-the-loop
HP	High pressure
IEPNEF	Intelligent Electric Power Network Evaluation Facility
LP	Low pressure
PMG	Permanent magnet generator
RTP	Real time platform
SRSG	Switched reluctance starter/generator
UAV	Uninhabited autonomous vehicle

II. INTRODUCTION

Uninhabited autonomous vehicles (UAVs) are being developed to undertake duties in a range of D-cubed (dangerous-dirty-dull) situations [1] for both civil and defence applications, with the earliest recorded UAV dating to the early 1900s [2]. More recently, larger concept demonstrators, such as the UK MoD-funded Taranis, have been announced [3]. Such large UAVs, with anticipated electrical power load levels in the region of 100kW, are likely to employ, and further develop, all-electric aircraft (AEA) concepts in which only electrical power is distributed throughout the aircraft as opposed to the conventional hydraulic, pneumatic, mechanical and electrical combination [4]. Therefore electrical solutions are needed for wing ice protection, actuators, flight control [5] and engine start [6]. To simplify further the engine power off-take, the generators are likely to be embedded in the core of the engine [6, 7]; one on the high-pressure (HP) spool, which must also act as a starter motor, and one on the low pressure (LP) spool. Robust fault-tolerant machines are essential such as switched reluctance [8] and multi-phase, high-output-impedance permanent magnet types [9]. Furthermore a common power bus architecture is needed to enable power sharing between the generators.

Hardware-in-the-loop (HIL) solutions are described in this paper to investigate the behaviour of a generic power system architecture for future UAVs; the start-up sequence and power sharing arrangements are of particular interest.

III. SYSTEM CONFIGURATION

The Intelligent Electric Power Network Evaluation Facility (IEPNEF) is being developed at the University of Manchester with Rolls-Royce funding using a combination of real hardware and HIL, where necessary, to enable the electrical system of a UAV to be investigated in a safe and controlled environment.

The IEPNEF contains a two-spool gas engine emulator system [10] with a 70kW 3,000rpm five-phase, fault-tolerant, permanent magnet generator (PMG) on the LP spool and a 30kW 15,000rpm switched reluctance starter/generator (SRSG) on the HP spool. Two variable-speed drives are used to emulate the engine spools. The HP spool drive has a regenerative capability to allow the emulation of electric engine starting. The speeds of the spool motor drives are commanded by the flight control system (FCS), a real-time platform (RTP) simulator that contains a model of the gas engine. In this work the spool speeds are programmed to follow pre-determined speed profiles, but a full gas engine model will be included in future work.

Two 30kW, 3kHz-bandwidth, bi-directional, DC/DC converter-based programmable active load systems (ALS) [10] are currently available to emulate both auxiliary power unit (APU) behaviour and other UAV load equipment such as electric actuators, fuel pumps and avionics. The load emulation is achieved by a RTP which runs a model of the actual load equipment and commands the DC/DC converters

The authors would like to thank Rolls-Royce plc for promoting and funding the Intelligent Electrical Power Network Evaluation Facility (IEPNEF) which is housed at The University of Manchester in the School of Electrical and Electronic Engineering.

to draw an appropriate current. The regeneration capability of the loads is an important feature as this enables models of electromechanical actuators to supply the bus with energy from the loaded surface [11], and also enables the behaviour of APU and energy storage devices to be emulated. Two 30kW resistive loads are available to represent background steady-state loads. A DC bus network, rated at 540V, connects the generators and load emulators.

The connection of the HP and LP gas engine emulators and generators, the active load systems, the resistor banks and the real-time simulation platforms are shown in Fig. 1. Power electronic converters are used to interface the variable frequency ac output of the generators to the 540V DC bus. The PMG is controlled using a real-time platform [12]. Contactors located in the power distribution network are used to enable system reconfiguration.

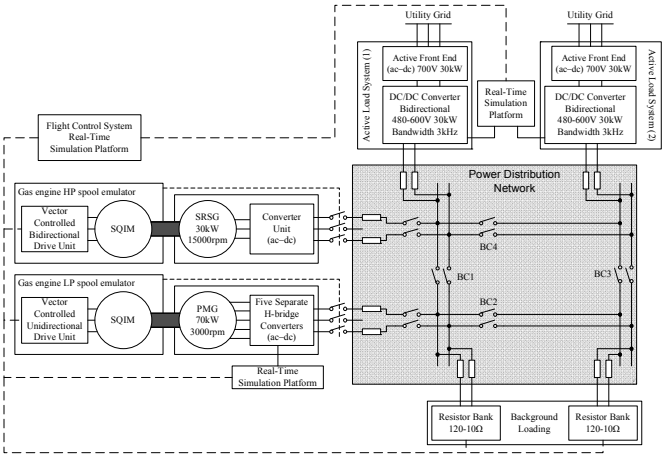

Fig. 1. IEPNEF configuration

The FCS also has the capability to schedule the load operation, enabling emulation of complete mission profiles and allowing power sharing or interaction effects to be studied.

IV. Load Sharing Control

To ensure orderly sharing of the electrical load by the two generators and the APU, the output voltage controller for each piece of equipment is programmed to have a droop profile as shown in Fig. 2.

The droop lines are all set to 20V at full generator/power supply output power; where the SRSG, PMG and APU nominal output powers are 30, 70 and 24.5kW respectively. Currently the closest available standard, MIL-STD-704F [13], on permissible DC bus voltage deviation is for a 270V DC bus and allows a variation in steady-state voltage of +10/-20V. In our case, for a 540V DC bus, if the allowed variation given in MIL-STD-704F [13] is doubled, then the maximum droop for all three items of equipment, APU, SRSG and PMG, will be within the +20/-40V variation.

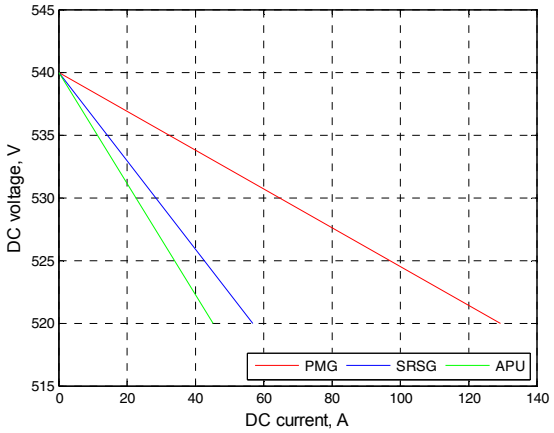

Fig. 2. APU, SRSG and PMG droop profiles

V. Start-Up Sequence

The start-up sequence for the gas engine and power network of an all-electric UAV, which can be demonstrated on the IEPNEF system (Fig. 1) is detailed in Fig. 3. Upon completion of the start-up sequence the UAV enters the flight stage.

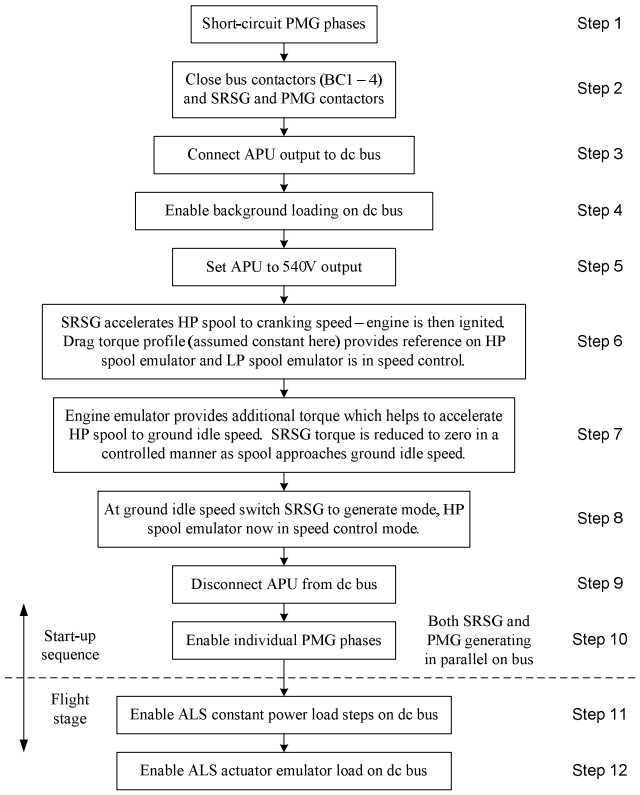

Fig. 3. Engine electric start sequence and system initialisation

The engine start sequence begins by priming the PMG ready for start-up by short-circuiting each phase; the lower transistors in each H-bridge leg are held on. The high phase impedance limits the current in the phases to the nominal

value of the machine, and uncontrolled rectification of the machine back emf onto the DC bus is prevented. As a result when the gas engine is accelerated to ground idle the PMG will be inactive and the only torque on the LP spool is friction and windage.

The bus and generator contactors, shown in Fig. 1, are then closed so that the capacitor bank of the SRSG and the PMG can be charged to the nominal voltage of 540V in a controlled manner by the APU. An APU, emulated using one of the ALS, is then connected to the bus. A background load of 60Ω is connected to the bus to represent the steady state behaviour of the electrical systems associated with the gas engine, which must be energised prior to ignition. The UAV bus system becomes live when the APU is started and the bus voltage is increased to 540V at a rate of 50V/s.

The SRSG, which is mounted on the HP spool, is then operated as a motor and is powered by the APU via the bus system. A drag torque is imposed on the SRSG during starting by the HP spool emulator. When the SRSG is at cranking speed the gas engine is ignited and starts to produce accelerating torque. As the HP spool accelerates towards ground idle speed the apparent drag torque falls to zero and the engine becomes self-sustaining. The SRSG is then switched from motoring to generating mode. Also as the HP spool accelerates to ground idle speed, the LP spool accelerates, bringing the PMG up to an operational speed, 1000rpm. Initially the SRSG and the APU are connected in parallel on the DC bus and the proportion of power supplied by each source is defined by the droop profiles shown in Fig. 2. The parallel operation enables no-break power transfer between the APU and SRSG.

The APU is then disabled and the PMG is connected in parallel with the SRSG making available the full power capacity of 100kW. The sharing of power between the two spools is again performed using a droop control method. The droop profile of the PMG is shown in Fig. 2. The PMG with all phases active will generate 2.27 times the output power of the SRSG; this is approximately the ratio between the nominal output power of the generators. When both generators are available on the DC bus the start-up sequence is complete and the system then enters a flight stage where the UAV loads vary with the mission profile.

VI. Experimental Results for Start-Up Sequence and Mission Profile

Results for the main stages of the start-up sequence, Fig. 3, are shown in the plots in Figs. 4 to 12. In each case the bus voltage and the current of the PMG, ALS and SRSG are presented. The first four steps of the start-up sequence prime both the PMG and the power system bus ready for start-up and then connect the APU and background loading to the bus. Once these stages have been completed the APU start-up, shown in Fig. 4, which is step 5 in Fig. 3 can be initiated.

In Fig. 4 the APU reference value starts at 50V for 1s before increasing at a rate of 50V/s to the final value of 536V, for a 60Ω load due to the droop line. The RTP runs an APU model enabling the output voltage to respond realistically to load changes. The APU current in Fig. 4 increases with voltage as a result of the fixed 60Ω of background loading. At approximately 8.5s the SRSG capacitor bank is automatically connected to the bus as part of the SRSG start-up routine; the capacitors being pre-charged to 350V before the contactor is closed. At t=11.8s the bus voltage is stable at 536V.

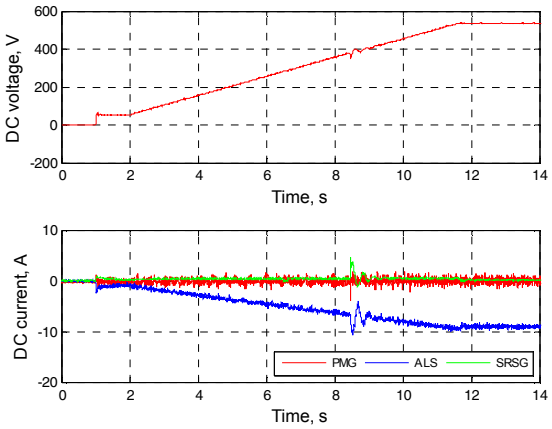

Fig. 4. APU start-up with a 60Ω load

Fig. 5 shows the SRSG accelerating the HP spool at a rate of 1000rpm/2.66s with a constant drag torque of 13Nm demanded by the gas engine emulator, step 6 in Fig. 3. More accurate gas engine modelling during starting will be included in future work.

The current consumed by the SRSG, Fig. 5, increases in proportion to the speed and settles at 20A at the cranking speed, 8000rpm. This variation in load present on the bus affects, via the droop line, the bus voltage magnitude.

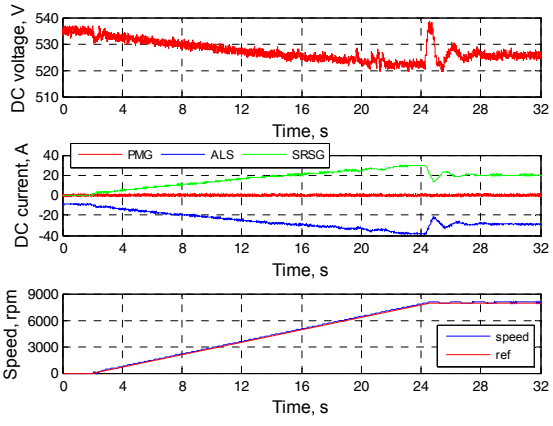

Fig. 5. SRSG motoring with 13Nm constant torque load on APU with 60Ω background load

The gas engine can then be ignited and the SRSG switched

to generate mode, step 8 in Fig. 3. The change in SRSG operation from motoring occurs at t=0.5s in Fig. 6.

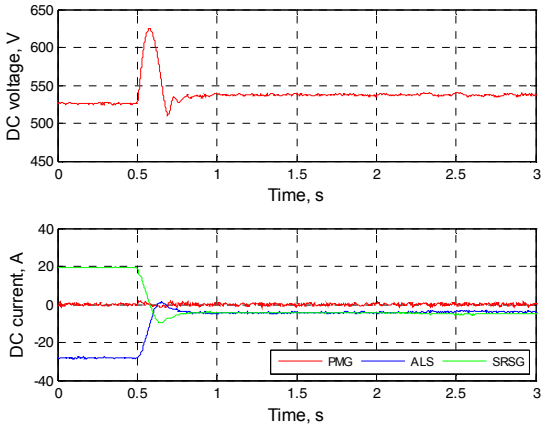

Fig. 6. SRSG motoring to generating transition with APU supplying bus with a constant 60Ω background load

The polarity of the SRSG current reverses as expected and the magnitude of the ALS current, operating as an APU, is reduced. The proportion of current generated by each power source on the bus, SRSG and APU, 5A and 4A respectively, is defined by the droop characteristics shown in Fig. 2. The voltage transient is due to the response of the APU voltage control loop when the approximately 5.5kW load of the motoring SRSG at 8000rpm is removed and replaced by a power source (the SRSG in generating mode) supplying the bus in parallel with the APU. The steady-state bus voltage is initially 526V in Fig. 6 when the APU is supplying both the background and SRSG motoring load. When the SRSG is switched to generate mode the bus voltage increases to 538V; as the load is now shared between the two power sources.

The APU is disabled at t=0.5s in Fig. 7, step 9 in Fig. 3.

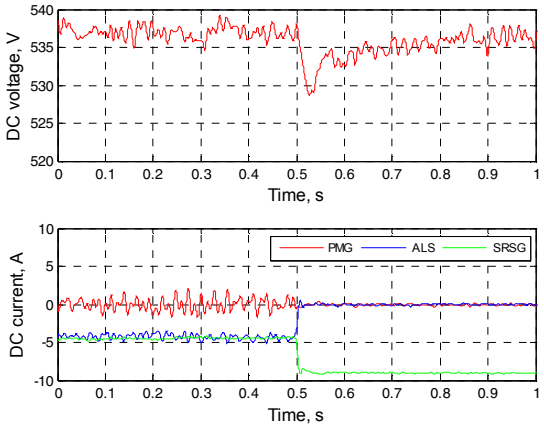

Fig. 7. APU disabled and SRSG supplying bus load

The output of the SRSG increases to supply the full 60Ω of background load. The bus voltage is slightly reduced when the load is supplied by a single source.

The final stage of the UAV start-up sequence in Fig. 3, step 10, is enabling the second generator, the 5-phase, fault-tolerant, PMG. As each phase is enabled in turn, the short-circuited current is reduced and brought under control, then the load angle is set according to the voltage control loop and droop profile.

The response of the bus voltage and the output DC currents of the SRSG and PMG are shown in Fig. 8 when the first phase is activated at t=0.5s; the remaining phases are still short-circuited.

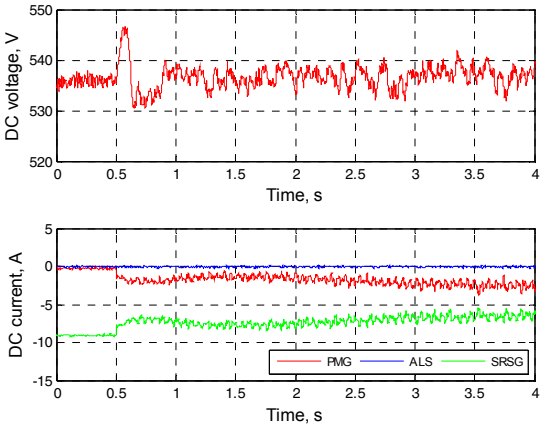

Fig. 8. SRSG and PMG connected in parallel supplying bus enable first phase of PMG 60Ω background load

At the instant the PMG phase is activated 1A of current is delivered to the bus which causes the SRSG output to decrease and a 10V transient in the bus voltage. The PMG control loops then regulate the PMG to deliver DC current. When a single phase of the PMG is active, with the remaining phases short circuited, the current output of the SRSG is defined by the droop profile in Fig. 2. Whereas the PMG droop line in Fig. 2 must be scaled so that the 20V drop is achieved at full per phase power. This results in a current share of 2.8A from the PMG and 6.2A from the SRSG. The initial values of the integral terms in the PMG control [12] are chosen for an intentionally slow response [14] to avoid disturbing the DC bus. Approximately 3s after the phase is enabled the two generator outputs settle to constant values.

The remaining phases of the PMG are activated in turn to minimise any disturbance on the bus. Once all the PMG phases are active then the full generation capability of 70kW is available on the bus. This signifies the end of the start-up sequence, shown in Fig. 3, and the UAV power system can be loaded according to the mission profile.

Three example load profiles have been included in this section to demonstrate the performance of the two generators when connected in parallel on a common DC bus.

Fig. 9 illustrates the response of the bus voltage and DC output of the two generators for cascaded steps in resistive load.

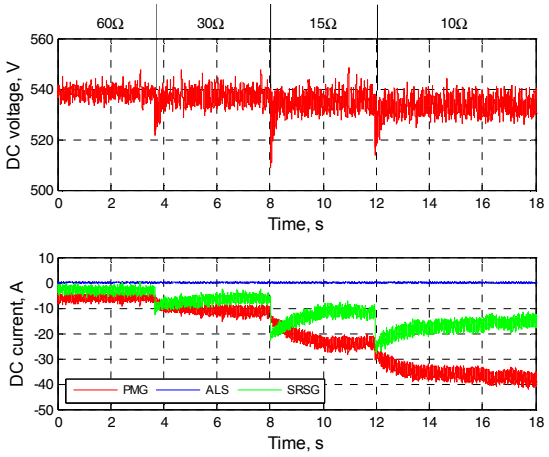

Fig. 9. Resistive load step changes

Initially the load is 60Ω, increasing to 30Ω at t=3.7s, 15Ω at t=8s and 10Ω at t=12s. This corresponds to power levels of approximately 4.85, 9.7, 19.4 and 29.1kW.

The bus voltage experiences a negative deviation due to the load increase, and decreases in magnitude due to the droop profiles. MIL-STD-704F [13] permits for a 270V DC bus system to drop 70V for 0.01s post transient and the permissible voltage deviation linearly reduces to 20V below the nominal 270V at 0.04s post transient. The most significant bus voltage deviation in Fig. 9 occurs at t=8s where the bus voltage drops initially to 509V and recovers to 525V 0.03s post transient and to 536V 0.35s post transient. The recovery of the nominal 540V bus voltage post transient is within the existing 270V MIL-STD-704F limits for the power transients considered here.

The DC current output of both generators increases as defined by the droop profiles, Fig. 2. The faster control response of the SRSG is evident in Fig. 9 as this generator initially responds to the increases in load and then settles to the predicted current share once the PMG control responds. The differing speed of the generator control loops helps to prevent interaction between the two generators.

To check further the power sharing and stability of the bus the ALS was programmed to impose a constant power load step of 4.8kW as shown at t=1s in Fig. 10. The DC output current of both generators varies with the load according to the droop characteristics, Fig. 2. The current share is 11A and 25A, for the SRSG and PMG respectively, with zero CPL and increase to 13A and 31A when the CPL is set to 4.8kW. The sum of the generator output currents is equal to the ALS current plus the current drawn by the 15Ω of background loading.

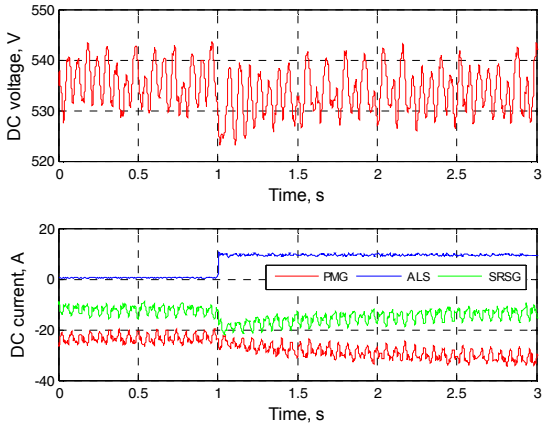

Fig. 10. Power step change (0 to 4.8kW) with 15Ω of background load

The final load profile imposed on the DC bus when both the PMG and the SRSG are connected in parallel is a 4kW electromechanical actuator model [15] that is executed on the ALS RTP. The actuator is commanded to open, 0.01m, and close every 5s with a duty ratio of 50%. The system response is shown in Fig. 11, and expanded in Fig. 12, to illustrate the detail of current drawn/supplied to the bus by the actuator model. A load of 15Ω is also present on the DC bus to represent background loads on the UAV. The pulses of actuator current are very short and are initially positive as the mechanical system starts to move and are then negative as the mechanical system is brought to rest. The small transients of regenerated power are absorbed by the DC bus without problem.

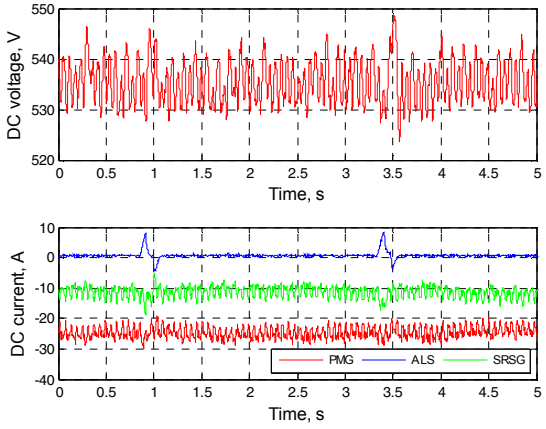

Fig. 11. Actuator model response with 15Ω of background loading

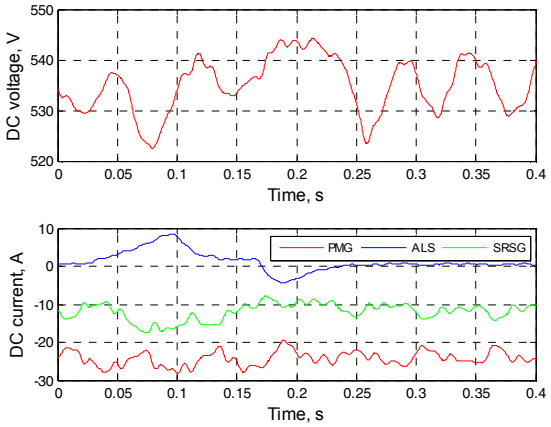

Fig. 12. Expanded view of actuator model response with 15Ω of background loading

VII. CONCLUSIONS

A detailed gas engine start-up sequence for an all-electric UAV employing embedded generators has been illustrated on a purpose built test facility employing HIL techniques. UAV start-up begins by connecting the generators to the bus so that the capacitors in the generator converters can be charged by the APU. The SRSG, mounted on the HP spool, is initially operated as a motor to accelerate the gas engine to ground idle at which point the gas engine is ignited and the SRSG is switched to generate operation. Initially the APU remains connected to the bus in parallel with the SRSG to ensure a no-break power transfer. The final stage of the engine start is to enable the LP spool mounted PMG. The pertinent steps of this engine start routine have been illustrated using test data. The UAV then enters the flight stage and sample test results have been included showing the response of the two generators connected in parallel for resistive and CPL steps, and actuator loads.

The experimental results demonstrate the system operation and focus on power quality and orderly power sharing and transfer between sources.

REFERENCES

[1] E. Pastor, J. Lopez, P. Royo, "UAV Payload and Mission Control Hardware/Software Architecture," IEEE Aerospace and Electronic Systems Magazine, Vol. 22, Issue 6, pp. 3-8, June 2007

[2] R. Schroer, "UAVs: The Future. [A Century of Powered Flight: 1903-2003]," IEEE Aerospace and Electronic Systems Magazine, Vol. 18, Issue 7, pp. 61-63, July 2003

[3] Taranis Unmanned Combat Air Vehicle (UCAV) Demonstrator, United Kingdom, http://www.airforce-technology.com/projects/tanaris, July 2009

[4] J.A. Weimer, "The Role of Electric Machines and Drives in the More Electric Aircraft," IEEE International Electric Machines and Drives Conference, 2003, Vol. 1, pp. 11-15, June 2003

[5] J.A. Rosero, J.A. Ortega, E. Aldabas, L. Romeral, "Moving Towards a More Electric Aircraft," IEEE Aerospace and Electronic Systems Magazine, Vol. 22, Issue 3, pp. 3-9, March 2007

[6] C.R. Avery, S.G. Burrow, P.H. Mellor, "Electrical Generation and Distribution for the More Electric Aircraft," 42nd International Universities Power Engineering Conference, UPEC 2007, pp. 1007-1012, Sept. 2007

[7] A.J. Mitcham, J.J.A. Cullen, "Permanent Magnet Generator Options for the More Electric Aircraft," IEE International Conference on Power Electronics, Machines and Drives (PEMD 2002), pp. 241-245, June 2002

[8] D.J. Powell, G.W. Jewell, S.D. Calverley, D. Howe, "Iron Loss in a Modular Rotor Switched Reluctance Machine for the 'More-Electric' Aero-Engine," Digests of the IEEE International Magnetics Conference, 2005 (INTERMAG Asia 2005), pp. 83–84, 4-8 April 2005

[9] J.E. Hill, S. Mountain, "Control of a Variable Speed, Fault Tolerant Permanent Magnet Generator," IEE International Conference on Power Electronics, Machines and Drives (PEMD 2002), pp. 492-497, June 2002

[10] F.J. Chivite-Zabalza, J. Calvignac, A.J. Forsyth, S. Long, D.R. Trainer, R. Todd, "Control and Development of an Electrical Systems Evaluation Platform for Uninhabited Autonomous Vehicles," 34th Annual Conference on IEEE Industrial Electronics, pp. 1479-1486, Nov. 2008

[11] D.R. Trainer, C.R. Whitley, "Electric Actuation-Power Quality Management of Aerospace Flight Control Systems," International Conference on (Conf. Publ. No. 487) Power Electronics, Machines and Drives, 2002, pp. 229-234, June 2002

[12] R. Todd, A.A. Abd Hafez, A.J. Forsyth, S.A. Long, "Single-Phase Controller Design for a Fault-Tolerant Permanent Magnet Generator," IEEE Vehicle Power and Propulsion Conference, VPPC '08, pp. 1-6, Sept. 2008

[13] Department of Defense (United States of America) Interface Standard, Aircraft Electric Power Characteristics, MIL-STD-704F, Mar. 2004

[14] R. Todd, A.J. Forsyth, "Control of Multi-Phase Fault-Tolerant PM Generator," UK Magnetics Society More Electric Aircraft One-Day Seminar, April 2009

[15] A.M. Cross, A.J. Forsyth, G. Mason. "Modelling and Simulation Strategies for the Electric Systems of Large Passenger Aircraft," *Society of Automotive Engineers Power Systems Conference*, No. 2002-01-3255, October 2002